Magnetic properties of quaternary Heusler alloys $Ni_{2-x}Co_xMnGa$

T. Kanomata,* Y. Kitsunai, and K. Sano
Faculty of Engineering, Tohoku Gakuin University, Tagajo 985-8537, Japan

Y. Furutani and H. Nishihara
Faculty of Science and Technology, Ryukoku University, Otsu 520-2194, Japan

R. Y. Umetsu and R. Kainuma
Institute of Multidisciplinary Research for Advanced Materials, Tohoku University, Sendai 980-8577, Japan

Y. Miura and M. Shirai
Research Institute of Electrical Communication, Tohoku University, Sendai 980-8577, Japan

(Received 15 April 2009; revised manuscript received 26 October 2009; published 3 December 2009; corrected 17 December 2009)

Magnetization and initial permeability measurements were done on the Heusler alloys $Ni_{2-x}Co_xMnGa$ ($0 \leq x \leq 2$). On the basis of the results, the magnetic-phase diagram was determined for $Ni_{2-x}Co_xMnGa$ ($0 \leq x \leq 2$). The Curie temperature T_C increases with increasing the Co concentration x. The martensitic transition temperature decreases abruptly with increasing x. The magnetic moment per formula unit at 5 K makes a broad maximum around $x=1.0$. The concentration dependence of the magnetic moment for $Ni_{2-x}Co_xMnGa$ ($0 \leq x \leq 2$) has been calculated using the Korringa-Kohn-Rostoker method. The computational results of the magnetic moment are in good agreement with the experimental results in this study.

DOI: 10.1103/PhysRevB.80.214402 PACS number(s): 75.50.Cc, 71.20.Be, 75.30.Cr

I. INTRODUCTION

In recent years, Heusler alloys have become the subject of intensive experimental and theoretical investigations. Ferromagnetic shape memory alloys (FSMAs) with Heusler structure have attracted much attention due to their potential application as smart materials.[1] They show large magnetic-field-induced strain by the rearrangement of twin variants in the martensite phase.[2] Unlike the case of conventional shape memory alloys, the speed of the shape change is not limited in this mechanism. Thus the ferromagnetic shape memory alloys are potential materials for a magnetomechanical actuator. Among them, Ni_2MnGa is the mostly studied alloy. Ni_2MnGa crystallizes in the cubic $L2_1$ Heusler structure and orders ferromagnetically at the Curie temperature $T_C \simeq 365$ K. On cooling below the martensitic transition temperature $T_M \simeq 200$ K, a superstructure forms, and the ferromagnetic state remains below T_M.[3,4] The electronic structures of Ni_2MnGa have been studied using the first-principles calculation by a number of authors,[5–11] especially reviewed by Entel *et al.*[12] According to the results of the calculations, Ni_2MnGa is a normal ferromagnet with both majority and minority bands crossing the Fermi level.

One of the unique properties of Heusler alloys is the half-metallic behavior. The characteristic electronic structures of the Co-based Heusler alloys, such as Co_2MnSn and Co_2MnAl, were early studied by Ishida *et al.*[13] and Kübler *et al.*[14] The existence of a gap in the minority-spin band structure leads to the 100% spin polarization of electronic state at the Fermi level and makes the half-metallic ferromagnets attractive for applications in the emerging field of spintronics. Since the discovery of the half metallicity for the Co-based Heusler alloys, a number of half-metallic ferromagnetic materials and their properties have been predicted by theoretical calculations and later verified by experiments. Especially, Co-based Heusler alloys have attracted considerable attention due to their easy growth and high Curie temperatures.[15] According to the results of calculations by Galanakis *et al.*,[16] Co_2MnGa is a ferromagnet with the high spin polarization.

To investigate the electronic properties of the ferromagnetic shape memory alloy Ni_2MnGa and the highly spin-polarized ferromagnetic alloy Co_2MnGa, we studied the magnetic properties of $Ni_{2-x}Co_xMnGa$ ($0 \leq x \leq 2$).

II. EXPERIMENTAL PROCEDURE

The polycrystalline $Ni_{2-x}Co_xMnGa$ ($0 \leq x \leq 2$) were prepared by the repeated melting of the appropriate quantities of the constituent elements, namely, 99.99% pure Ni, 99.95% pure Mn, 99.9% pure Co, and 99.9999% pure Ga, in an argon arc furnace. Subsequently samples were sealed in the evacuated double silica tubes, heated at 1073 K for three days and then quenched in water. We needed further annealing three times in the temperature range from 1073 to 1273 K to achieve the high crystalline perfection for the samples with $x=0.3$, 0.5, 1.0, and 2.0. The phase identification and characterization of the samples were carried out by x-ray diffraction measurements using Cu-$K\alpha$ radiation. Magnetization M data were collected using a commercial superconducting quantum interference device magnetometer in fields up to 50 kOe. The temperature dependence of the initial permeability was measured using ac method under the applied magnetic field of about 7 Oe. A vibrating sample magnetometer was used to determine the Curie temperature at high temperatures. The order-disorder transition temperature T_t from the $L2_1$ phase to the $B2$ phase was determined by a differential scanning calorimeter.

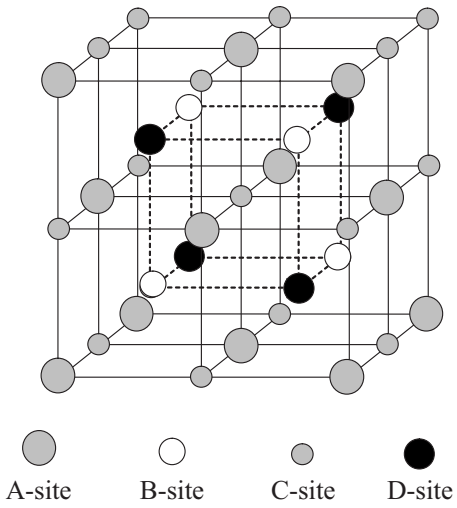

FIG. 1. Unit cell of the Heusler-type alloy. The sites are presented by A, B, C, and D.

III. RESULTS AND DISCUSSIONS

A. Experimental results

All samples prepared in this study were shown to crystallize in the $L2_1$ structure at room temperature by the x-ray powder-diffraction measurements. The $L2_1$ structure may conveniently be considered as four interpenetrating fcc sublattices with A, B, C, and D sites. The A, B, C, and D sites are located at (0, 0, 0), (1/4, 1/4, 1/4), (1/2, 1/2, 1/2), and (3/4, 3/4, 3/4), respectively, as shown in Fig. 1. In Ni_2MnGa, Ni atoms occupy the A and C sites, and Mn atoms and Ga atoms the B and D sites, respectively. Replacing Ni with Co in Ni_2MnGa, Co atoms occupy the A and C sites randomly. Figure 2 shows the concentration dependence of the lattice parameter a at room temperature of $Ni_{2-x}Co_xMnGa$ ($0 \leq x \leq 2$). The lattice parameter decreases linearly with increasing the concentration x, which may be attributed to the difference in the ionic radii of the Ni and Co atoms. The lattice parameters of Ni_2MnGa and Co_2MnGa are found to be 5.825 and 5.768 Å, respectively. These values are in good agreement with those reported earlier.[4,17]

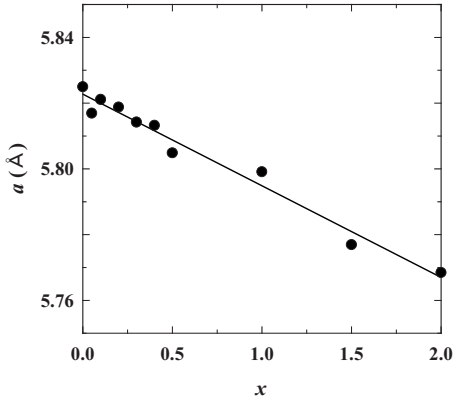

FIG. 2. Lattice parameter a versus concentration x curve for $Ni_{2-x}Co_xMnGa$ ($0 \leq x \leq 2$) alloys at room temperature. Solid line in the figure is a guide for the eyes.

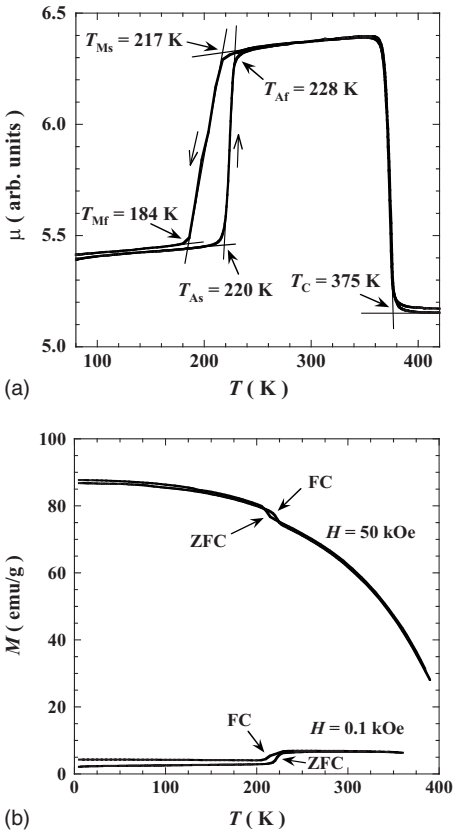

FIG. 3. (a) Temperature dependence of the initial permeability μ for $Ni_{1.95}Co_{0.05}MnGa$. T_{Ms} and T_{Mf} mean the martensitic transition starting and finishing temperatures, respectively. T_{As} and T_{Af} indicate the reverse martensitic transition starting and finishing temperatures, respectively. T_C is the Curie temperature. (b) Thermomagnetization curves of $Ni_{1.95}Co_{0.05}MnGa$ in a ZFC and a FC processes at 0.1 and 50 kOe.

The temperature dependence of the initial permeability μ for $Ni_{1.95}Co_{0.05}MnGa$ ($x=0.05$) is shown in Fig. 3(a). The abrupt changes in μ are observed around 200 K for cooling and heating processes. These temperature dependence of μ are similar to those of FSMAs $Ni_2Mn_{1-x}Fe_xGa$ ($0.0 \leq x \leq 0.7$).[18] So, these temperature variations in μ correspond to transition between the martensite phase and the austenite phase. The martensitic transition starting and finishing temperatures T_{Ms} and T_{Mf}, and reverse martensitic transition starting and finishing temperatures T_{As} and T_{Af} were defined as the cross point of the linear extrapolation lines from both higher and lower temperature ranges on the μ versus T curves as shown in the figure. The arrows along the curves in Fig. 3(a) show the heating and cooling processes. The abrupt decrease in μ at high temperature corresponds to the transition from the ferromagnetic state to the paramagnetic state. The Curie temperature was also defined as the cross point of the linear extrapolation lines from higher and lower temperature ranges on the μ versus T curve. The Curie temperature is found to be 375 K for $Ni_{1.95}Co_{0.05}MnGa$. Similar μ versus T curves are observed for all samples with $0 \leq x \leq 0.2$. For the samples with $0.2 < x \leq 1.0$, μ decreases sharply with increasing temperature only around T_C. Figure 3(b) shows the temperature dependence of the magnetization M measured in

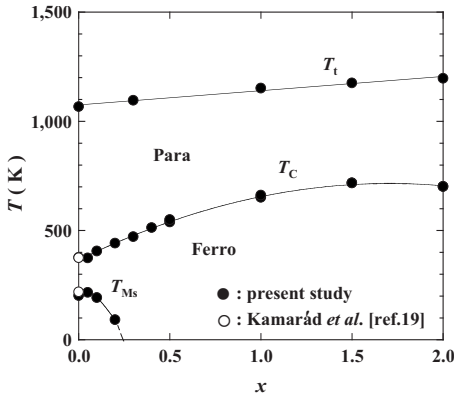

FIG. 4. Phase diagram of $Ni_{2-x}Co_xMnGa$ alloys, where Para and Ferro mean paramagnetic and ferromagnetic states, respectively. T_{Ms} indicates the martensitic transition starting temperature. T_C and T_t mean the Curie temperature and the $B2/L2_1$ order-disorder transition temperatures, respectively.

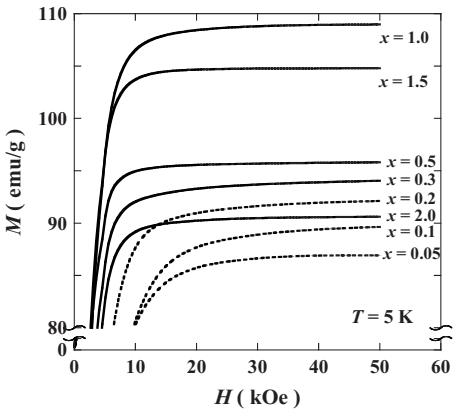

FIG. 5. Magnetization curves at 5 K for $Ni_{2-x}Co_xMnGa$ alloys with various concentration x. Magnetization curves for the samples in the martensite phase are shown by dotted lines.

a zero-field-cooling (ZFC) and a field-cooling (FC) processes at applied fields of 0.1 and 50 kOe for $Ni_{1.95}Co_{0.05}MnGa$. The curves on the bottom correspond to $H=0.1$ kOe. The martensitic transition is accompanied by an abrupt change in M because the lower symmetry of the martensite phase enhances the magnetocrystalline anisotropy energy. As seen in Fig. 3(b), we observe a small jump of M in a field of 50 kOe around the martensitic transition temperature with decreasing temperature. At $H=50$ kOe, M is saturated for $Ni_{1.95}Co_{0.05}MnGa$ as shown later. This means that the magnetic moment per formula unit of the martensite phase is larger than that of the austenite phase. We have carried out precise magnetization and initial permeability measurements for samples with various concentration x in $Ni_{2-x}Co_xMnGa$ $(0 \leq x \leq 2)$ besides the sample with $x=0.05$. Based on these experimental results and the reported data for $x=0.0$,[19] the magnetic-phase diagram of $Ni_{2-x}Co_xMnGa$ $(0 \leq x \leq 2)$ was determined as shown in Fig. 4. The Curie temperature increases with increasing x and tends to saturate. This may be attributed to the strong coupling between Co and Mn atoms. Indeed, Kurtulus *et al.*[20] confirmed on the basis of first-principles calculations that the exchange coupling between Co and Mn atoms is dominant in Co_2MnGa and related Heusler alloys and is much larger than that between Ni and Mn atoms in Ni_2MnSn. On the other hand, T_{Ms} decreases sharply with increasing x. The sample with $x=0.30$ did not show the martensitic transition in the temperature range from 5 to 500 K. Some authors showed that the martensitic transition temperature for the ternary FSMAs with the $L2_1$ structure depends strongly on the average number of valence electrons per atom e/a.[21–25] The martensitic transition starting temperature T_{Ms} increases significantly and linearly with increasing e/a. Some authors revealed that this empirical linear relationship between T_{Ms} and e/a holds even for the quaternary Ni-Mn-V-Ga,[21] Ni-Mn-Ga-Ge,[21] and $Ni_2Mn_{1-x}Co_xGa$ $(0.0 \leq x \leq 0.188)$ FSMAs.[23] Here, it was assumed that the number of valence electrons per atom for Ni, Co, Mn, V, Ge, and Ga atoms are $10(3d^8 4s^2)$, $9(3d^7 4s^2)$, $7(3d^5 4s^2)$, $5(3d^3 4s^2)$, $4(4s^2 4p^2)$, and $3(4s^2 4p^1)$, respectively. These configurations correspond to the periodic table and are commonly used in band calculations of the electronic structure for Heusler alloys. We expect that T_{Ms} of $Ni_{2-x}Co_xMnGa$ $(0 \leq x \leq 2)$ decreases with increasing x from the empirical relationship of T_{Ms} and e/a. The experimental result in this study is in good accordance with our expectation. On the other hand, the $B2/L2_1$ order-disorder transition temperature T_t increases linearly with increasing x.

According to the Bragg-Williams-Gorsky approximation, if the X atom perfectly occupies its own site, the T_t of the X_2YZ is given by the following simple equation:[26,27]

$$T_t = \frac{3}{2k} W_{yz}^{(2)}, \tag{1}$$

where $W_{yz}^{(2)}$ is the interchange energy of Y-Z bonds in the second nearest neighbors and k is Boltzmann's constant. This equation means that the T_t proportional to the $W_{yz}^{(2)}$ should be constant if the $W_{yz}^{(2)}$ is independent of the kind of the host X atoms. However, it has been recently reported that the T_t of X_2TiAl (X=Fe, Co, Ni, and Cu) Heusler alloys shows a linear relation to the concentration of valence electron c_e of X site atoms and that the $W_{yz}^{(2)}$ considerably depends on the kind of the host X atoms.[27] The linear behavior of the T_t in the present X_2MnGa (X=Co and Ni) alloys is similar to that of the X_2TiAl alloys, while the T_t of the Ni_2MnGa with a higher c_e is slightly lower than that of the Co_2MnGa with a lower c_e. The origin of such effects of the host X atoms on the T_t of the X_2TiAl and X_2MnGa Heusler alloys is not clear and theoretical investigations are required.

The magnetization curves at 5 K for $Ni_{2-x}Co_xMnGa$ with various concentration x are shown in Fig. 5. All of the magnetization curves are characteristic of ferromagnetism. The magnetization at 5 K for the samples with $0.0 \leq x \leq 0.2$ is saturated in a field of about 20 kOe. On the other hand, the magnetization at 5 K for the samples with $0.3 \leq x \leq 1.0$ is saturated in a field of about 10 kOe. The magnetization of samples in the austenite phase is easy to be saturated compared to that in the martensite phase due to the difference in the magnetocrystalline anisotropy energy. The spontaneous magnetization at 5 K for $Ni_{2-x}Co_xMnGa$ $(0 \leq x \leq 2)$ was determined by the linear extrapolation to $H/M=0$ of the M^2

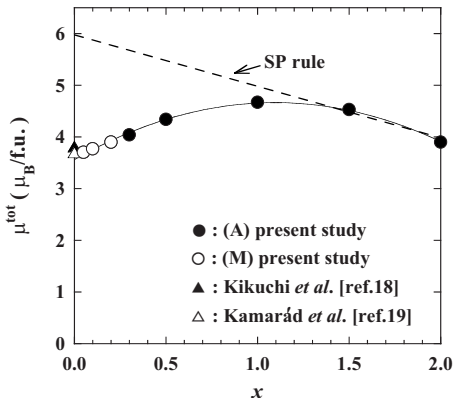

FIG. 6. Concentration dependence of the magnetic moment per formula unit, μ^{tot}, at 5 K for $Ni_{2-x}Co_xMnGa$ alloys. The open circles and the filled circles correspond to μ^{tot} at 5 K for the samples in the martensite phase and in the austenite one, respectively. A and M in the figure mean the austenite phase and the martensitic phase, respectively. The SP rule is demonstrated by a broken line in the figure.

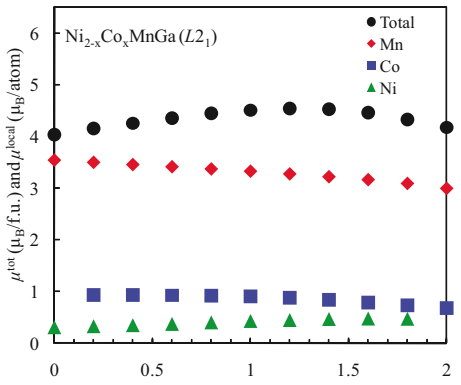

FIG. 7. (Color online) The total magnetic moment per formula μ^{tot} (circle points) and the local magnetic moment per atom μ^{local} (diamond points for Mn, square points for Co, and triangle points for Ni) as a function of x in $Ni_{2-x}Co_xMnGa$.

versus H/M curves. The magnetic moment per formula unit at 5 K, μ^{tot}, for $Ni_{2-x}Co_xMnGa$ ($0 \leq x \leq 2$) was estimated from the spontaneous magnetization and is plotted against the concentration x as shown in Fig. 6. The magnetic moment increases with increasing x and makes a broad maximum around $x=1.0$.

B. Theoretical results

Ni_2MnGa is the normal ferromagnetic metal with both majority and minority bands crossing the Fermi level as mentioned above. On the other hand, Co_2MnGa is highly spin-polarized ferromagnet with the spin polarization value of 81%.[25] More recently, Umetsu *et al.*[28] also calculated the total density of states of Co_2MnGa by the linear muffin-tin orbital method with the atomic sphere approximation. In order to clarify the effects of Ni substitution for Co to the magnetic moment of $Ni_{2-x}Co_xMnGa$, we performed electronic-structure calculations of $L2_1$-type $Ni_{2-x}Co_xMnGa$ on the basis of the Korringa-Kohn-Rostoker method[29] developed by Akai,[30] where the atomic disorder is included within the coherent-potential approximation. We adopt the generalized gradient approximation[31] for the exchange and correlation term. We use the lattice constants $a_{Ni2MnGa}-(a_{Ni2MnGa}-a_{Co2MnGa})x/2$ for $Ni_{2-x}Co_xMnGa$, where $a_{Ni2MnGa}=5.80$ Å and $a_{Co2MnGa}=5.71$ Å are obtained in the optimized calculations for Ni_2MnGa and Co_2MnGa, respectively. Our results are obtained by the so-called scalar-relativistic calculation, in which the spin-orbit interaction is neglected. It is considered that the spin-orbit interaction does not play an important role to the magnetic moment of $Ni_{2-x}Co_xMnGa$ because considerably small orbital moments (~ 0.025 μ_B for Ni and ~ 0.016 μ_B for Mn) compared to the spin moments are reported in the full-relativistic calculations of Ni_2MnGa.[32]

Figure 7 presents the calculated total magnetic moment per formula μ^{tot} and the local magnetic moment per atom μ^{local} as a function of x in the $Ni_{2-x}Co_xMnGa$ ($0 \leq x \leq 2$). The calculated μ^{tot} in Fig. 7 is in good accordance with the experimental results in Fig. 6. For half metal, the total magnetic moment μ^{tot} follows Slater-Pauling (SP) behavior, being the number of the valence electrons in the unit cell −24.[16] Co_2MnGa has the μ^{tot} very near the ideal 4 μ_B predicted by the SP rule as shown in Fig. 6. The local magnetic moment μ^{local} of Co and Mn in Fig. 7 increases by the Ni substitution for Co, indicating that the substitution of Ni for Co in Co_2MnGa increases the electrons in the majority states around Co and Mn. This leads the increase in the μ^{tot} toward the ideal 6 μ_B according to the SP rule for Ni_2MnGa as demonstrated with a broken line in Fig. 6. As is shown in Fig. 7, the Mn spin moment increases with decreasing x as like the SP rule because the lattice expansion of $Ni_{2-x}Co_xMnGa$ by the Ni substitution for Co enhances localization of spin density around Mn. However, the μ^{tot} deviates from the SP rule and decreases with decreasing x for $x \lesssim 1.5$. The decrease in the μ^{tot} can be attributed to the decrease in the local magnetic moment of Ni by the Ni substitution for Co as shown in Fig. 7 owing to the smaller exchange splitting of Ni than that of Co and Mn.

We show in Fig. 8 the total density of states (DOS) and the local density of states (LDOS) of the $Ni_{2-x}Co_xMnGa$ for $x=1.6$, 1.0, and 0.4. The spin polarization monotonically decreases with increasing the Ni concentration in the $Ni_{2-x}Co_xMnGa$ (34% for $x=1.6$, −18% for $x=1.0$, and −27% for $x=0.4$), reflecting the small spin polarization of the $L2_1$-type Ni_2MnGa. In the case of $x=1.6$ (Co-rich case), the DOS and the LDOS still have a dip structure around the Fermi level in the minority-spin state originated from the second nearest-neighbor Co($d\gamma$)-Co($d\gamma$) hybridization, leading the SP-like behavior of the μ^{tot}. In the case of $x=1.0$ and $x=0.4$ (Ni-rich case), the dip around the Fermi level in the minority-spin sates shifts toward the lower-energy side and the Ni($d\gamma$) states are partially occupied. Since the second nearest-neighbor Ni($d\gamma$)-Ni($d\gamma$) hybridization provides the small energy gap compared to that of Co($d\gamma$)-Co($d\gamma$), the further substitution of Ni for Co in the Ni-rich $Ni_{2-x}Co_xMnGa$ alloys may lead to the decrease in the gap in the minority band, namely, the decrease in μ^{tot} as well as the spin polarization.

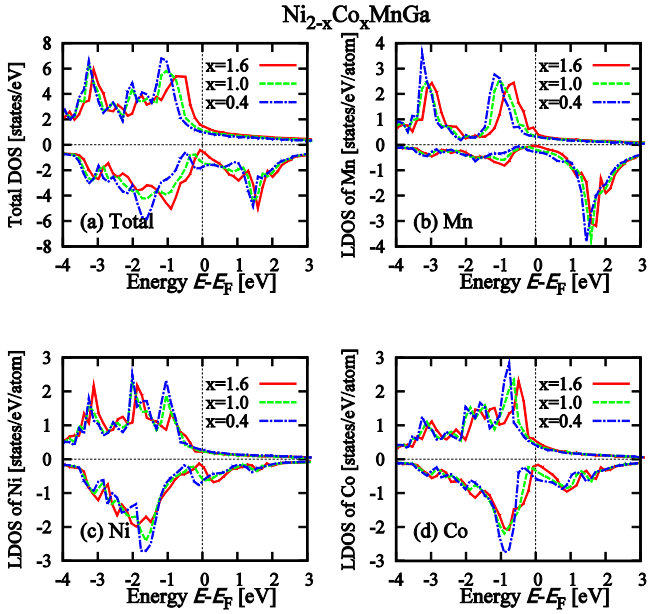

FIG. 8. (Color online) (a)Total DOS and local DOS of (b) Mn, (c) Ni, and (d) Co for $x=1.6$ (solid lines), $x=1.0$ (broken lines), and $x=0.4$ (dotted broken lines) of $Ni_{2-x}Co_xMnGa$ as a function of energy relative to the Fermi energy. The positive and negative signs of the DOS and the LDOS indicate the majority-spin and minority-spin states, respectively.

IV. CONCLUSION

Magnetization and initial permeability measurements were carried out on the Heusler alloys $Ni_{2-x}Co_xMnGa$ ($0 \leq x \leq 2$). On the basis of the experimental results, the magnetic-phase diagram of $Ni_{2-x}Co_xMnGa$ ($0 \leq x \leq 2$) was determined. The Curie temperature increases with increasing x. This may be attributed to the strong coupling between Mn and Co atoms. The martensitic transition temperature decreases abruptly with increasing x and the martensite phase collapses at $x \simeq 0.25$. The magnetic moment per formula unit at 5 K makes a broad maximum around $x=1.0$. The magnetic moment of $Ni_{2-x}Co_xMnGa$ ($0 \leq x \leq 2$) has been calculated using the Korringa-Kohn-Rostoker method. The substitution of Ni for Co in Co_2MnGa increases the electrons in the majority states around Co and Mn. This leads the increase in the μ^{tot} toward the ideal 6 μ_B according to the SP rule for Ni_2MnGa. However, the μ^{tot} deviates from the SP rule and decreases with decreasing x for $x \lesssim 1.5$. This decrease in the μ^{tot} can be attributed to the decrease in the local magnetic moment of Ni by the Ni substitution for Co owing to the smaller exchange splitting of Ni than that of Co and Mn. The computational results of the magnetic moment are in good agreement with the experimental results in this study.

ACKNOWLEDGMENTS

The authors would like to thank A. Kimura of Graduate School of Science, Hiroshima University for valuable discussions. This work was partly supported by a Cooperative Research Project Program of RIEC, Tohoku University. This work was also partly supported by a grant based on the High-Tech Research Center Program for private universities from the Japan Ministry of Education, Culture, Sports, Science and Technology. This work was also partly supported by a Grant-in-Aid for Scientific Research (Grant No. 21560693), provided by the Japan Society for the Promotion of Science.

*Corresponding author; kanomata@tjcc.tohoku-gakuin.ac.jp

[1] A. Planes, L. Mañosa, and A. Saxena, *Magnetism and Structure in Functional Materials* (Springer-Verlag, Berlin, 2005).
[2] K. Ullakko, J. K. Huang, C. Kantner, R. C. O'Handley, and V. V. Kokorin, Appl. Phys. Lett. **69**, 1966 (1996).
[3] P. J. Webster, K. R. A. Ziebeck, S. L. Town, and M. S. Peak, Philos. Mag. B **49**, 295 (1984).
[4] P. J. Brown, J. Crangle, T. Kanomata, M. Matsumoto, K.-U. Neumann, B. Ouladdiaf, and K. R. A. Ziebeck, J. Phys.: Condens. Matter **14**, 10159 (2002).
[5] S. Fujii, S. Ishida, and S. Asano, J. Phys. Soc. Jpn. **58**, 3657 (1989).
[6] A. Ayuela, J. Enkovaara, K. Ullakko, and R. M. Nieminen, J. Phys.: Condens. Matter **11**, 2017 (1999).
[7] V. V. Godlevsky and K. M. Rabe, Phys. Rev. B **63**, 134407 (2001).
[8] A. Ayuela, J. Enkovaara, and R. M. Nieminen, J. Phys.: Condens. Matter **14**, 5325 (2002).
[9] Y. Tanaka, S. Ishida, and S. Asono, Mater. Trans. **45**, 1060 (2004).
[10] E. Şaşıoğlu, L. M. Sandratskii, and P. Bruno, Phys. Rev. B **70**, 024427 (2004).
[11] S. R. Barman, S. Banik, and A. Chakrabarti, Phys. Rev. B **72**, 184410 (2005).
[12] P. Entel, V. D. Buchelnikov, V. V. Khovailo, A. T. Zayak, W. A. Adeagbo, M. E. Gruner, H. C. Herper, and E. F. Wassermann, J. Phys. D: Appl. Phys. **39**, 865 (2006).
[13] S. Ishida, A. Akazawa, Y. Kudo, and J. Ishida, J. Phys. F: Met. Phys. **12**, 1111 (1982).
[14] J. Kübler, A. R. Williams, and C. B. Sommers, Phys. Rev. B **28**, 1745 (1983).
[15] *Half-metallic Alloys: Fundamentals and Applications*, Lecture Notes in Physics, edited by I. Galanakis and P. H. Dederichs (Springer-Verlag, Berlin, 2005), Vol. 676.
[16] I. Galanakis, P. H. Dederichs, and N. Papanikolaou, Phys. Rev. B **66**, 174429 (2002).
[17] P. J. Webster, J. Phys. Chem. Solids **32**, 1221 (1971).
[18] D. Kikuchi, T. Kanomata, Y. Yamaguchi, H. Nishihara, K. Koyama, and K. Watanabe, J. Alloys Compd. **383**, 184 (2004).
[19] J. Kamarád, F. Albertini, Z. Arnold, F. Casoli, L. Pareti, and A. Paoluzi, J. Magn. Magn. Mater. **290-291**, 669 (2005).
[20] Y. Kurtulus, R. Dronskowski, G. D. Samolyuk, and V. P. Antropov, Phys. Rev. B **71**, 014425 (2005).
[21] V. A. Chernenko, Scr. Mater. **40**, 523 (1999).
[22] X. Jin, M. Marioni, D. Bono, S. M. Allen, R. C. O'Handley, and T. Y. Hsu, J. Appl. Phys. **91**, 8222 (2002).

[23] H. Nakamura, K. Tsuchiya, and M. Umemoto, Trans. Mater. Res. Soc. Jpn. **26**, 287 (2001).
[24] T. Krenke, X. Moya, S. Aksoy, M. Acet, P. Entel, L. Mañosa, A. Planes, Y. Elerman, A. Yücel, and E. F. Wasserman, J. Magn. Magn. Mater. **310**, 2788 (2007).
[25] M. Sargolzaei, M. Richter, K. Koepernik, I. Opahle, H. Eschrig, and I. Chaplygin, Phys. Rev. B **74**, 224410 (2006).
[26] G. Inden, Z. Metallkd. **66**, 648 (1975).
[27] K. Ishikawa, R. Kainuma, I. Ohnuma, K. Aoki, and K. Ishida, Acta Mater. **50**, 2233 (2002).
[28] R. Y. Umetsu, K. Kobayashi, A. Fujita, R. Kainuma, K. Ishida, K. Fukamichi, and A. Sakuma, Phys. Rev. B **77**, 104422 (2008).
[29] W. Kohn and N. Rostoker, Phys. Rev. **94**, 1111 (1954).
[30] H. Akai, J. Phys.: Condens. Matter **1**, 8045 (1989).
[31] M. Rasolt and D. J. W. Geldart, Phys. Rev. B **34**, 1325 (1986).
[32] J. Enkovaara, A. Ayuela, J. Jalkanen, L. Nordström, and R. M. Nieminen, Phys. Rev. B **67**, 054417 (2003).